



Published in final edited form as:

Anal Chem. 2010 April 15; 82(8): 3383–3388. doi:10.1021/ac9024335.

Increasing the Sensitivity of ELISA using Multiplexed Electrokinetic Concentrator

Lih Feng Cheow¹, Sung Hee Ko², Sung Jae Kim¹, Kwan Hyoung Kang², and Jongyoon Han^{*,1,3}

¹Department of Electrical Engineering and Computer Science, Massachusetts Institute of Technology, 77 Massachusetts Avenue, Cambridge, Massachusetts 02139

²Department of Mechanical Engineering, San 31, Pohang University of Science and Technology, Hyoja-dong, Pohang, Korea 790-784

³Department of Biological Engineering, Massachusetts Institute of Technology, 77 Massachusetts Avenue, Cambridge, Massachusetts 02139

Abstract

We developed a novel method to increase the sensitivity of standard Enzyme-Linked Immunosorbent Assay (ELISA) using a multiplexed electrokinetic concentration chip. The poly(dimethylsiloxane) (PDMS) molecular concentrator¹ was used to trap and collect charged fluorescent product of target-bound enzyme turnover reaction of ELISA that occurred in a standard 96 well plate. Detection sensitivities of both Prostate Specific Antigen (PSA) and CA 19-9 (a human pancreatic and gastrointestinal cancer marker) ELISAs in serum are enhanced ~100 fold with a low CV of <17%. We also integrated this method with an on-chip bead-based ELISA that lends itself toward a fully-automated on-chip diagnostic device. Detection sensitivity of microfluidic bead-based CA 19-9 ELISA in serum is enhanced ~65 fold compared to the results without electrokinetic accumulation step. This chip can be directly applied to enhance the readout sensitivity of a wide range of existing ELISA kits at concentrations below the current detection limit.

INTRODUCTION

One of the most pressing issues in analytical chemistry is detecting low abundance analytes from complex samples such as blood. Tests for low abundance biomarkers such as human prostate specific antigen (PSA) and human pancreatic and gastrointestinal cancer marker (CA 19-9) are routinely used for initial tumor screening, to monitor patient response during cancer therapy, and to help detect recurrence following treatment^{2, 3}. Therefore, there is significant clinical relevance to increase the sensitivity of these tests to facilitate early detection of the onset and recurrence of cancer, since these biomarkers get diluted significantly in blood, especially in early stages of the disease progression. Among various new and old immunoassay formats, ELISAs (Enzyme-Linked Immunosorbent Assays) are probably the most widely-used techniques, due to their simplicity, flexibility and the enzymatic signal amplification enabling high sensitivity⁴. Still, the ultimate detection sensitivity of ELISA is not good enough to tackle the challenges of biomarker detection. This led to the development of many novel ultrasensitive immunoassay platforms⁵⁻⁸. However, additional sensitivity comes with the cost of added complexity in amplification chemistry or complicated readout devices. Being able to measure analytes at concentrations below the current detection limits of ELISA, without modifying the

* To whom correspondence should be addressed. jyhan@mit.edu Phone: +1-617-253-2290. Fax: +1-617-258-5846 .

basic workflow of ELISA (therefore applicable to any existing ELISA setup), would be very useful.

Our group has developed nanofluidic preconcentration devices that can be used to continuously collect and trap charged molecules in a given sample into a much smaller volume, thereby increasing local concentration significantly^{1, 9}. These devices have been used to enhance surface-bound protein binding kinetics¹⁰ as well as to increase the sensitivity of homogeneous enzyme assay^{11, 12}. While these methods demonstrated superior sensitivity, they were tailored for the specific molecules and need to be optimized for concentrating other molecules. Furthermore, these devices were not demonstrated in a multiplexed format.

In this paper, we utilize a multiplexed nanofluidic electrokinetic concentrator to accumulate fluorescent product molecules from ELISA in a small volume. Instead of aiming to affect the primary immunobinding by concentrating binding partners¹⁰, here we simply aim to collect the fluorescent product of standard ELISA complex, without modifying the immunobinding process of ELISA. By increasing the local concentration of reporter molecule by several orders of magnitude at the detection zone, we achieved ~65-100 fold enhancements in detection limit of two cancer markers. We also demonstrated multiplexing capability by performing concentration-enhanced ELISA of cancer biomarkers from five different samples concurrently, thus enabling us to obtain a dose response curve in one single experiment. Since the same substrate can be used for a whole range of ELISA kits, the same device can be directly applied to immunoassay of different analytes. As a proof of concept, we performed our experiment with two cancer markers, PSA and CA 19-9, which are two important biomarkers in cancer diagnostic and post treatment monitoring^{2, 3}.

I. CONCENTRATION ENHANCED MICROWELL ELISA

EXPERIMENTAL SECTION

Microchip Fabrication—The microchip was fabricated using poly(dimethylsiloxane) PDMS (Sylgard 184, Dow Corning Inc., Midland, MI) irreversibly bonded on a glass slide. Microchannels were molded in PDMS by replica molding technique¹³. To obtain the positive master mold, the desired design was photolithographically patterned onto a silicon wafer using positive photoresist. Next, the wafer was etched to a depth of 15 μm via a reactive ion etching (RIE) process. The silicon master was further treated with trichlorosilane (T2492, UCT Specialties, Bristol, PA) in a vacuum desiccator overnight to prevent adhesion to PDMS.

We fabricated the ion-selective nanoporous structures by using the microflow patterning technique to obtain a thin strip of Nafion film on a standard glass slide^{1, 11}. A 50 μm deep and 400 μm wide PDMS microchannel was used to define the flow path of the Nafion solution (20 wt% solution in lower aliphatic alcohol/H₂O mix, Sigma Aldrich, St. Louis, MO). The PDMS chip with microchannels was irreversibly bonded on top of the glass slide by standard plasma bonding.

Materials—We tested our microfluidic chip on two commercially available ELISA kits for common biomarkers. The first was a human prostate serum antigen (PSA) ELISA kit (Catalog #8425-300, Monobind Inc., Lake Forest, CA). The second kit was a human pancreatic and gastrointestinal cancer marker (CA 19-9) ELISA kit (Catalog #1840, Alpha Diagnostics International Inc., San Antonio, TX).

We used Amplex Red (A12222, Invitrogen Corp., Carlsbad, CA) as the fluorogenic enzyme substrate. This colorless substrate reacts with hydrogen peroxide with a 1:1 stoichiometry to produce highly fluorescent resorufin¹⁴ (excitation/emission maxima = 570/585 nm). FITC dye (F143, Invitrogen Corp., Carlsbad, CA) was used as a tracer to monitor electrokinetic

accumulation under a different filter set (excitation/emission maxima = 490/513 nm). Donkey serum was obtained from Innovative Research, Novi, MI. Electrokinetic product accumulation was done in 0.01X PBS with pH 7.4 as the buffer solution.

Sample Preparation—Immunobinding reaction of PSA and CA 19-9 was performed in donkey serum and control serum prepared from human sera respectively. Twenty five μL of serially diluted antigen sample in serum was added to a 100 μL mixture of biotinylated primary antibody and HRP-coupled secondary antibody in a Streptavidin coated microwell strip. After 60 minutes incubation at room temperature, the microwell contents were discarded by decantation and washed six times with wash buffer. Finally, 100 μL of freshly prepared substrate solution (containing 20 μM Amplex Red, 10 μM H_2O_2 , and 100 μM FITC tracer in 0.01X PBS buffer) was added to all wells. After 30 minutes incubation, the contents of the wells were collected in separate microcentrifuge tubes and used immediately or stored at -20°C and thawed to room temperature before using.

Device Scheme and Operation—A schematic of the multiplexed PDMS concentrator is shown in Figure 1. The chip contained five sample loading inlets connected to one common outlet. See Supplementary Material for the fabricated device. Two side channels flanked the inlet channels to provide symmetrical electrical ground. An ion-selective nanojunction was fabricated at the center of the device to concentrate the fluorescent product molecules by electrokinetic trapping when voltages were applied. We have also fabricated arrays of pillar structures in front of the nanojunction, which helped to stabilize the location of the electrokinetically trapped molecules by reducing vortexes formed in the ion depletion zone during concentration polarization¹⁵.

Figure 2a showed a detailed operation of the device. Conventional ELISA was performed entirely in microwell strips as described in the sample preparation section. Next, reaction products corresponding to different antigen concentrations were loaded into each inlet channels.

To electrokinetically trap the charged fluorescent enzymatic product molecules, we applied 30 V to all the inlet and outlet reservoirs for 10 minutes, while grounding the side channels. An ion depletion region was induced near the ion-selective Nafion membrane by concentration polarization effect^{16, 17}. Meanwhile, liquid height difference between the inlet and outlet reservoirs (15 μL sample in inlet reservoirs, 10 μL buffer in outlet reservoir) induced a gravitational flow that continuously stacked the charged enzyme product molecules against the ion depletion zone. We performed this experiment three times in the same device to investigate intraassay repeatability. Between each experiment, the channels were flushed with deionized water for 5 minutes to remove carryover from the previous experiment.

Measurement Instrument and Image Analysis—An inverted epifluorescence microscope IX 71 (Olympus, Center Valley, PA) equipped with a cooled CCD camera (SensiCam, Cooke Corp., Romulus, MI) was used for fluorescence imaging. A mechanical shutter (Olympus, Center Valley, PA), which only opens for 100 ms when images are taken, was used to prevent photobleaching of the fluorescent molecules. It had been reported that strong excitation light led to enzyme independent autocatalyzed photooxidation of Amplex Red to fluorescent resorufin¹⁸. We took images every 5 s and engaged two neutral density filters (ND6) during imaging to reduce this effect. The images were analyzed using the NIH ImageJ software. Nonuniformity in background signal was corrected by subtracting an image of the device filled with deionized water taken before each experiment. To quantify the concentrated product molecules, we plotted a profile of the channel-width-averaged fluorescence intensity and picked the maximum value. To quantify the product molecules without electrokinetic accumulation, we measured the channel-width-averaged fluorescence

intensity in a region far before the concentrated plug. Origin7 software (OriginLab Corp., Northampton, MA) was used to fit the dose response curve.

RESULTS AND DISCUSSION

Mechanism of Multiplexed Electrokinetic Accumulation—The overall design of multiplexed electrokinetic accumulation was different from previously reported, single-gate or double-gate devices^{1, 9-12}. In the multiplexed devices shown in this paper, not all the sample channels were directly adjacent to a grounded side channel, yet electrokinetic accumulation still occurred in each channel, with approximately the same efficiency (checked by monitoring FITC accumulation). We believe that there were alternative paths through the ion selective membrane directly connecting each sample channel to the side channels. In the microflow patterning method^{1, 11}, the 400 μm wide planar Nafion membrane was found to be $\sim 1 \mu\text{m}$ thick by surface profiling. Cations from the inner sample channels could travel within the Nafion matrix to the outermost side channels. Further experiments are being conducted now to verify this hypothesis.

Multiplexed Concentration Enhanced ELISA—We spiked donkey serum with known amounts of PSA (1000 pg/mL, 200 pg/mL, 40 pg/mL, 8 pg/mL, 1.6 pg/mL) to simulate the effect of a complex sample matrix. Conventional ELISA of these samples was performed in microwell strips, and the enzymatic reaction was allowed to proceed for 30 minutes. After this, the enzymatic products were injected into the microchip for electrokinetic accumulation. Figure 2b showed uniform accumulation of the tracer molecule, which indicated similar accumulation rate. Tracer molecules at the top channel accumulated at a different location from the rest of the channels because the high concentration of charged product molecules modified the ionic environment at the vicinity of the nanojunction¹⁹ (Figure 2b). Figure 2c showed electrokinetic accumulation of enzymatic product molecules of PSA ELISA. Without electrokinetic accumulation, only the top channel, which corresponded to high PSA concentration (1000 pg/mL), showed visible product fluorescence. However, the fluorescence intensity in all five channels was markedly increased in the accumulation zone. Figure 2d showed the dose response curve of PSA ELISA in both normal mode and accumulation mode. The error bars represented one standard deviation for three separate experiments. As it was unclear the effect of electrokinetic accumulation on the dose response curve, we fitted it to a second order polynomial equation. Zero-dose response was obtained by simultaneous accumulation of zero-dose ELISA products in three channels. The limit of detection (LOD) corresponds to the analyte concentration needed to produce a signal three standard deviations above the zero dose response. Using this criterion, the LOD of PSA ELISA with electrokinetic accumulation was 1.85pg/mL, compared to 193.5pg/mL without electrokinetic accumulation, representing ~ 100 -fold sensitivity enhancement.

To show that this method is general and can be applied to multiple analyte, we performed a similar experiment using CA 19-9 as the target antigen. We spiked human control serum with known amount of CA 19-9 (6.25 U/mL, 1.25 U/mL, 0.25 U/mL, 0.05 U/mL and 0 U/mL) and repeated the above experiment. The result (SI Figure 2 in Supplementary Material) showed the dose response curve of CA 19-9 ELISA in both normal mode and accumulation mode. The LOD of CA 19-9 ELISA with electrokinetic accumulation was 0.011 U/mL, compared to 1.2 U/mL without electrokinetic accumulation, representing ~ 110 -fold sensitivity enhancement.

II. CONCENTRATION ENHANCED ON-CHIP BEAD BASED ELISA

Realization of point-of-care (POC) testing is difficult with conventional immunoassay, since rather large devices are necessary for automated practical diagnosis systems²⁰. A fully automated portable micro-ELISA system is recently demonstrated as a viable POC tool²¹. In micro-ELISA, immunobinding reaction occurs at the surface of polystyrene beads that are

captured within the microchannel. Dye molecules produced by enzymatic reaction upon introduction of substrates are detected downstream of the bead capture zone. However, micro-ELISA suffers from poor sensitivity in continuous-flow condition due to the short enzymatic reaction time²¹. Higher sensitivity could be achieved in the stop-flow mode²¹, but even in this case the signal intensity levels off due to equilibrium of dye molecule production and diffusion.

We can provide a simple solution to this problem by accumulating the dye molecules downstream of the reaction zone using an electrokinetic concentrator. This would make micro-ELISA a powerful ultrasensitive POC diagnostic tool, applicable to a wide range of low abundance targets. As a proof of concept, we performed concentration enhanced bead-based ELISA of the cancer marker CA 19-9.

EXPERIMENTAL SECTION

Sample Preparation—Twenty fives μL of serially diluted antigen sample in control serum, 50 μL of the biotinylated primary antibody, and 5 μL of Streptavidin coated beads (Applied Biosystems, Foster City, CA) were added into a microcentrifuge tube and mixed by vortexing. After 60 minutes incubation at room temperature, the tubes were spun in a centrifuge for 5 minutes at 6000 rpm to obtain a firm pellet of beads. The supernatant was discarded and the pellet was resuspended in 100 μL of wash buffer. This step was repeated five times to ensure proper washing. Next, 50 μL of the HRP-coupled secondary antibody solution was added into each tube and incubated for 60 minutes at room temperature, followed by six washing steps as described above. Finally, the beads were resuspended in 100 μL 0.01X PBS buffer.

Device Scheme and Operation—Figure 3a showed a detailed procedure and the operation of the device in each inlet channel. Beads from different samples were loaded into each inlet reservoirs, and a negative pressure was applied at the outlet reservoir to pull in the bead solution. Since the diameter of the beads (6 – 8 μm) was larger than the gaps between the pillar structures (5 μm), the beads were trapped in front of the pillar structures. Negative pressure was removed when the length of the bead pack reached $\sim 500 \mu\text{m}$ ($\pm 15\%$). Following this, the bead solution in the inlet reservoir was removed and flushed with deionized water for 30 seconds.

In the second step, freshly prepared substrate solution (containing 20 μM Amplex Red, 10 μM H_2O_2 , and 100 μM FITC tracer in 0.01X PBS buffer) was injected into the inlet reservoirs. Electrokinetic trapping of charged fluorescent product molecules was similar to the previous experiment, with a 20 V potential difference between the inlet channels and side channels, and gravitational flow due to 40 μL sample in the inlet reservoirs vs. 20 μL buffer in the outlet reservoir. We performed this experiment three times in the same device using the same parameters to investigate intraassay repeatability. Between each experiment, the channels were flushed with deionized water for 5 minutes to remove carryover from the previous experiment.

RESULTS AND DISCUSSION

Multiplexed Concentration Enhanced Bead-Based ELISA—Figure 3 showed simultaneous accumulation of ELISA products for beads incubated with serial dilution (6.25 U/mL, 1.25 U/mL, 0.25 U/mL, 0.05 U/mL and 0 U/mL) of CA 19-9 in control serum. Uniform bead packing was achieved in all five channels. From Figure 3b, only the top channel which contains beads with high surface concentration of antigen appeared slightly fluorescent immediately after the beads, indicating the low assay sensitivity. However, at the vicinity of the nanojunction, electrokinetic trapping led to accumulation of the charged fluorescent product molecules and clear increase in signal intensity in all five channels. Figure 3c showed the dose response curve of CA 19-9 ELISA in both normal mode and accumulation mode, fitted to a second order polynomial equation. The LOD of CA 19-9 ELISA with electrokinetic

accumulation was 0.02 U/mL, compared to 0.13 U/mL without electrokinetic accumulation, representing approximately 65 fold sensitivity enhancement.

Repeatability Studies—Repeatability of immunoassay is an important figure of merit, since it is directly related to the issues of false-positive and false-negative biomarker detection, both with serious clinical consequences. We characterized the intra-assay reproducibility of the multiplexed concentration enhanced ELISA by measuring the coefficient of variation (CV). We calculated the CV as the standard deviation σ divided by the mean fluorescence μ of three separate experiments for biomarker concentration ($CV = \sigma/\mu$). As shown in Table 1, the CV of microwell PSA and CA 19-9 ELISA with electrokinetic accumulation was below 17% across the entire dynamic range, showing good reproducibility of our assay. In comparison, the maximum CV for bead based CA 19-9 ELISA was 37%. We attribute the increase in CV to the variation of the number of beads ($\pm 15\%$) in each channel, which leads to different hydrodynamic resistance and enzymatic reaction time. It had been reported that the substrate turnover efficiency in an enzymatic packed bead reactor is a function of flow rate²². Hence, variations in bead packing could lead to errors in microfluidic bead based ELISA. Secondly, due to variable zeta potential in the differently functionalized beads in each channel, different electroosmotic flow was induced in each channel. Furthermore, beads could be dislodged from the bead trap due to backpressure generated during electrokinetic accumulation of charged molecules.

Comparison with ELISA on a Plate Reader—Finally, we compared our results with conventional fluorogenic readout on a 96 well plate reader (Varioskan Flash, Thermo Scientific, Waltham, MA). Table 2 shows the comparison among the ELISA LOD's obtained in the electrokinetic accumulation region, in the microchannel without electrokinetic accumulation, and in a 96 well plate. Electrokinetic accumulation improves the PSA/CA 19-9 ELISA detection sensitivity by $\sim 100X/110X$ compared to fluorogenic detection in microchannel without electrokinetic accumulation, and $\sim 30X/10X$ compared to plate reader. The microchannel detection is least sensitive due to its short optical path length (12 μm) compared to that of 96 well plate ($\sim 2\text{mm}$).

The detection limit of CA 19-9 bead based ELISA in a microchannel without electrokinetic accumulation (0.13 U/mL) was slightly better to that obtained in a 96 well plate (0.115 U/mL). This is attributed to the high enzymatic conversion efficiency at the bead pack and confinement of the fluorescent product to the downstream of the microchannel²³. With electrokinetic accumulation, the detection sensitivity was $\sim 70X$ better than both cases.

CONCLUSION

In this paper, we reported a novel multiplexed PDMS microfluidic platform to improve the readout sensitivity of fluorogenic ELISA. An ion-selective membrane patterned across the microchannels enabled electrokinetic accumulation of charged fluorescent ELISA products, thereby increasing local signal intensity in the trapping zone. Up to five assays could be performed simultaneously in a multiplexed format, enabling assay parallelization for high-throughput immunoassay.

The post-ELISA accumulation step presented here could find wide applications for low abundant biomolecule detection such as disease marker, cytokines, hormones, and specific analytes in biological research. In this method, the enzyme substrate that is used here can be applied to all other HRP-based ELISA without any modification. Hence there is no need to re-develop the assay for a new analyte. The method presented here could capitalize on the tremendous amount of validation and quality control performed by ELISA kit manufacturers to produce results with high reproducibility while extending the dynamic range of

immunoassay towards a lower limit. Due to the simplicity of fabrication and small sample volume requirement, this microchip is amenable to direct integration with lab-on-chip devices to provide automation and new capabilities such as single-cell immunoassay.

Supplementary Material

Refer to Web version on PubMed Central for supplementary material.

Acknowledgments

This work was supported by NIH (CA119402 and EB005743). L.F. Cheow is supported by the A*STAR National Science Scholarship. S.H. Ko is supported by the Korea Science and Engineering Foundation grant (R0A-2007-000-20098-0). Microfabrication of the device was done in the Microsystems Technology Laboratories of MIT, with the help of its staff members.

REFERENCES

- (1). Lee JH, Song Y-A, Han, J. *Lab Chip* 2008;8:596–601.
- (2). Steinberg W. *The American journal of gastroenterology* 1990;85:350. [PubMed: 2183589]
- (3). Catalona W, Smith D, Ratliff T, Dodds K, Coplen D, Yuan J, Petros J, Andriole G. *New Engl. J. Med* 1991;324:1156. [PubMed: 1707140]
- (4). Wild, D. *The Immunoassay Handbook*. 3rd ed. Elsevier Ltd.; 2005.
- (5). Zheng G, Patolsky F, Cui Y, Wang WU, Lieber CM. *Nat. Biotechnol* 2005;23:1294–1301. [PubMed: 16170313]
- (6). Schweitzer B, Wiltshire S, Lambert J, O'Malley S, Kukanskis K, Zhu Z, Kingsmore SF, Lizardi PM, Ward DC. *Proc. Natl. Acad. Sci. U. S. A* 2000;97:10113–10119. [PubMed: 10954739]
- (7). Wu G, Datar R, Hansen K, Thundat T, Cote R, Majumdar A. *Nat. Biotechnol* 2001;19:856–860. [PubMed: 11533645]
- (8). Nam J-M, Thaxton CS, Mirkin CA. *Science* 2003;301:1884–1886. [PubMed: 14512622]
- (9). Wang Y-C, Stevens AL, Han J. *Anal. Chem* 2005;77:4293–4299. [PubMed: 16013838]
- (10). Wang Y-C, Han J. *Lab Chip* 2008;8:392–394. [PubMed: 18305855]
- (11). Lee JH, Song Y-A, Tannenbaum SR, Han J. *Anal. Chem* 2008;80:3198–3204. [PubMed: 18358012]
- (12). Lee J, Cosgrove B, Lauffenburger D, Han J. *J. Am. Chem. Soc* :803–812.
- (13). Duffy DC, McDonald JC, Schueller OJA, Whitesides GM. *Anal. Chem* 1998;70:4974–4984.
- (14). Zhou M, Diwu Z, Panchuk-Voloshina N, Haugland R. *Anal. Biochem* 1997;253:162–168. [PubMed: 9367498]
- (15). Ko, SH.; Kim, SJ.; Kang, KH.; Han, J. *MicroTAS 2009*. Jeju, Korea: 2009. p. 168-170.
- (16). Kim SJ, Wang Y-C, Lee JH, Jang H, Han J. *Phys. Rev. Lett* 2007;99:044501. [PubMed: 17678369]
- (17). Probstein, RF. *Physicochemical Hydrodynamics : An Introduction*. Wiley-Interscience; 1994.
- (18). Gorris H, Walt DJ. *Am. Chem. Soc* 2009;131:6277–6282.
- (19). Humble PH, Kelly RT, Woolley AT, Tolley HD, Lee ML. *Anal. Chem* 2004;76:5641–5648. [PubMed: 15456281]
- (20). Sato K, Yamanaka M, Takahashi H, Tokeshi M, Kimura H, Kitamori T. *Electrophoresis* 2002;23
- (21). Ohashi T, Mawatari K, Sato K, Tokeshi M, Kitamori T. *Lab Chip* 2009;9:991–995. [PubMed: 19294312]
- (22). Seong GHS, Heo J, Crooks RM. *Anal. Chem* 2003;75:3161–3167. [PubMed: 12964765]
- (23). Sato K, Yamanaka M, Hagino T, Tokeshi M, Kimura H, Kitamori T. *Lab Chip* 2004;4:570–575. [PubMed: 15570367]

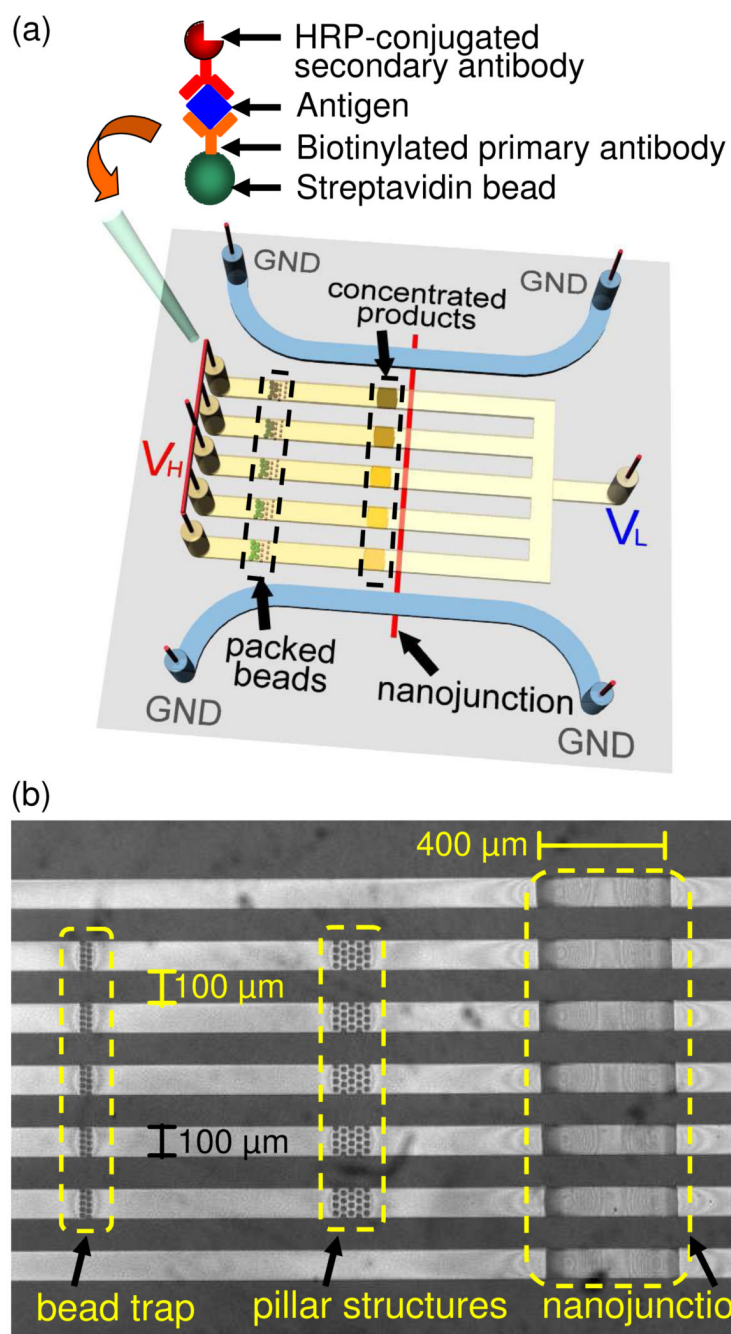


Figure 1.

(a) Schematic of the multiplexed electrokinetic accumulator, which consists of a Nafion nanojunction that spans the five inlet microchannels and two side channels. Sandwich ELISA was performed on 6-8 μm Streptavidin beads, which were then loaded sequentially into the inlet reservoirs. (b) Microscope image of the fabricated PDMS microchannels integrated with a surface patterned nanojunction.

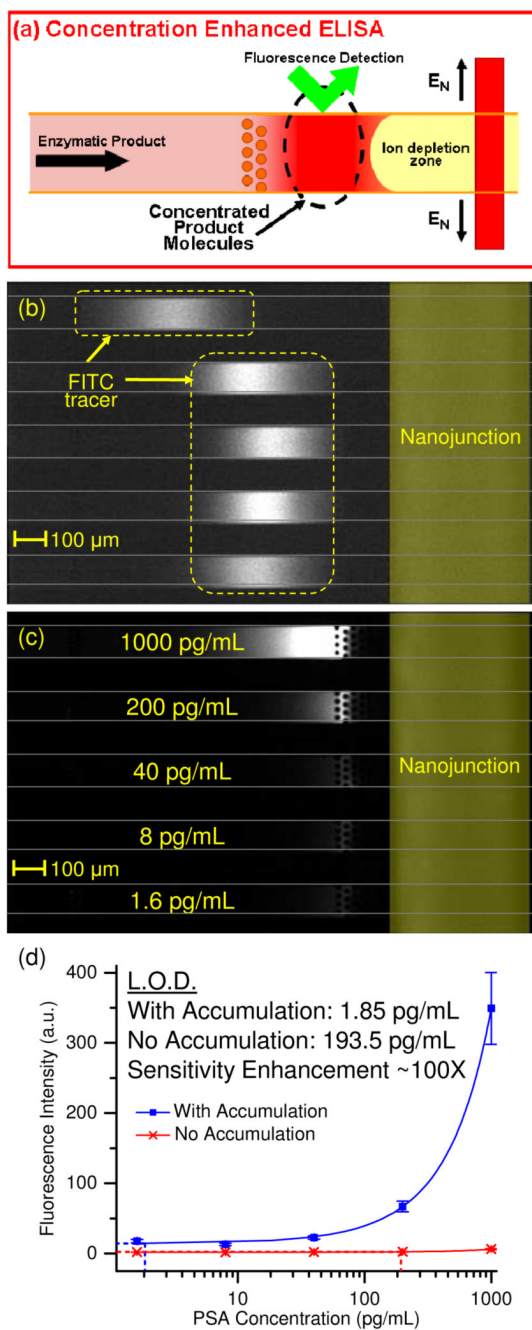


Figure 2. Concentration-enhanced PSA ELISA. (a) ELISA product from 96-well plates was directly injected into the microchannels. When a voltage was applied between the inlet microchannels and the side channels, the product molecules were electrokinetically accumulated and attained a high local concentration. The sensitivity of fluorescence detection was significantly enhanced in this region. (b) The concentrated FITC tracer showed similar intensities, indicating similar accumulation rate in all channels. (c) Without electrokinetic accumulation, only the top channel (corresponding to high concentration of PSA) displayed a slight increase in product fluorescence. In the accumulation region, it was easy to differentiate the difference in product fluorescence between each channel. (d) Dose response curve of concentration enhanced PSA

ELISA. Square markers represent intensities with product accumulation, while cross markers represent intensities without product accumulation. Error bars indicate one standard deviation from the mean of three separate experiments. Sensitivity enhancement due to product accumulation was ~ 100 fold.

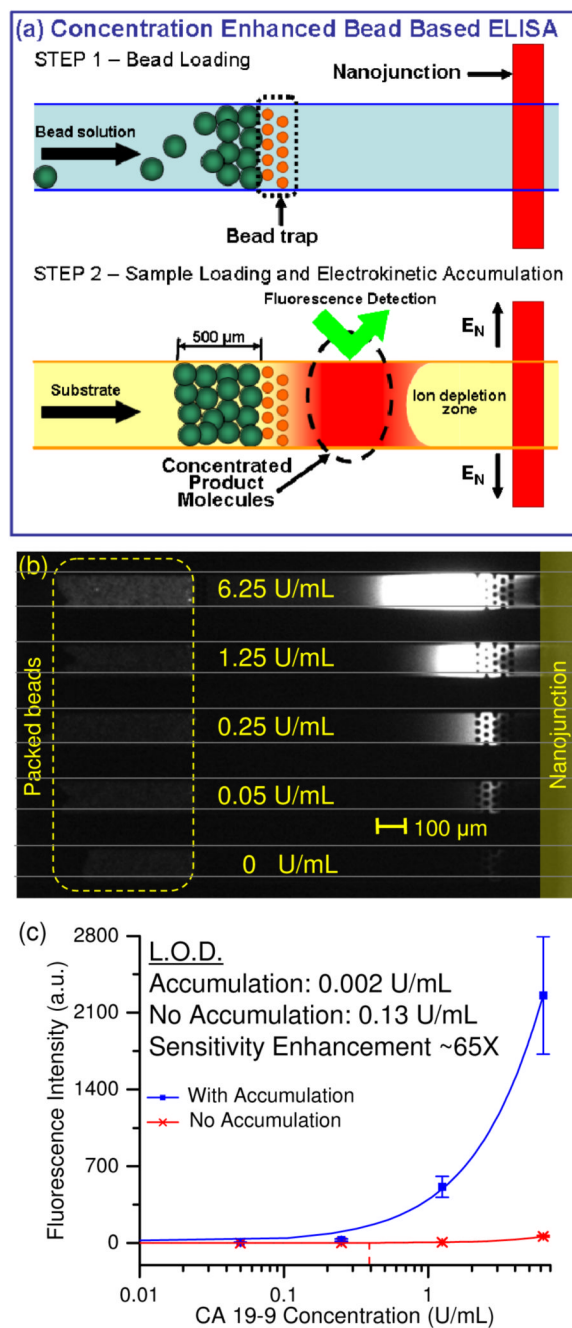


Figure 3.

Concentration-enhanced bead based CA 19-9 ELISA. (a) Step 1: Functionalized beads were drawn into the inlet microchannels by applying a negative pressure at the outlet reservoir. The 6-8 μm beads were trapped in front of the 5 μm microfabricated constrictions. Step 2: Substrate molecules were injected into the inlet microchannels, and were enzymatically converted into charged fluorescent product molecules in the bead pack. When a voltage was applied between the inlet microchannels and the side channels, the product molecules were electrokinetically accumulated and attained a high local concentration. The sensitivity of fluorescence detection was significantly enhanced in this region. (b) Without electrokinetic accumulation, only the top channel which contained beads with high surface concentration of antigen displayed visible

increase in product fluorescence. In the accumulation region, it was easy to differentiate the difference in product fluorescence between each channel. (c) Dose response curve of concentration enhanced bead based CA 19-9 ELISA. Square markers represent intensities with product accumulation, while cross markers represent intensities without product accumulation. Sensitivity enhancement due to product accumulation was ~ 65 fold.

Table 1

Coefficients of variation for PSA and CA 19-9 ELISA in accumulation mode.

PSA Concentration (pg/mL)	1000	200	40	8	1.6
CV (%) (Concentration Enhanced ELISA)	14.6	11.4	9.9	12.7	14.6
CA 19-9 Concentration (U/mL)	6.25	1.25	0.25	0.05	0
CV (%) (Concentration Enhanced ELISA)	6.2	2.0	1.7	16.5	8.4
CV (%) (Bead Based Concentration Enhanced ELISA)	23.7	18.7	37.2	33.6	7.5

Table 2

Comparing the limit of detection of PSA and CA 19-9 between different methods.

Limit of Detection (LOD)	Microchannel (Electrokinetic Concentration)	Microchannel (No Electrokinetic Concentration)	96 well Plate
PSA in Donkey Serum (Concentration Enhanced ELISA)	1.85 pg/mL	193.5 pg/mL	64 pg/mL
CA 19-9 in Control Serum (Concentration Enhanced ELISA)	0.011 U/mL	1.2 U/mL	0.115 U/mL
CA 19-9 in Control Serum (Bead Based Concentration Enhanced ELISA)	0.002 U/mL	0.13 U/mL	0.115 U/mL